View metadata, citation and similar papers at core.ac.uk

brought to you by CORE

provided by Open Archive Toulouse Archive Ouverte

Open Archive Toulouse Archive Ouverte (OATAO)

OATAO is an open access repository that collects the work of Toulouse researchers and makes it freely available over the web where possible.

This is an author-deposited version published in: http://oatao.univ-toulouse.fr/
Eprints ID : 2761

To link to this article :
URL : http://dx.doi.org/10.1111/j.1551-2916.2007.01485.x

To cite this version : Elissalde, C. and Maglione, M. and Estournès, Claude (2007) *Tailoring Dielectric Properties of Multilayer Composites Using Spark Plasma Sintering.* Journal of the American Ceramic Society , vol. 90 (n° 3). pp. 973-976. ISSN 0002-7820

Any correspondence concerning this service should be sent to the repository administrator: staff-oatao@inp-toulouse.fr

DOI: 10.1111/j.1551-2916.2007.01485.x

Tailoring Dielectric Properties of Multilayer Composites Using Spark Plasma Sintering

Catherine Elissalde[†] and Mario Maglione

Institut de Chimie de la Matière Condensée de Bordeaux-CNRS, Université Bordeaux I, 33608 Pessac, France

Claude Estournès

CIRIMAT et Plateforme Nationale CNRS de Frittage Flash, PNF2 MHT, Université Paul Sabatier, 33062 Toulouse, France

A straightforward and simple way to produce well-densified ferroelectric ceramic composites with a full control of both architecture and properties using spark plasma sintering (SPS) is proposed. SPS main outcome is indeed to obtain high densification at relatively low temperatures and short treatment times thus limiting interdiffusion in multimaterials. Ferroelectric/dielectric (BST64/MgO/BST64) multilayer ceramic densified at 97% was obtained, with unmodified Curie temperature, a stack dielectric constant reaching 600, and dielectric losses dropping down to 0.5%, at room-temperature. This result ascertains SPS as a relevant tool for the design of functional materials with tailored properties.

I. Introduction

The need for functional materials in numerous fields of applications, biology, nanotechnology, and electronics has stimulated the research in tailored materials design. Processing ferroelectric polycrystalline materials with controlled properties is relevant to obtain promising candidates for microelectronics and telecommunication devices.[1–3] Driven by the applications of ferroelectric materials for multilayer ceramic capacitors and tunable devices such as phase shifters, an intense research effort has focused on composite materials including both a ferroelectric and a non-ferroelectric oxide.[4–6] The mixed perovskite $Ba_{0.6}Sr_{0.4}TiO_3$ (BST64) is an attractive candidate as its ferroelectric transition occurs close to room temperature, however, it displays strong temperature sensitivity and high-frequency dielectric losses. To overcome these drawbacks, composites based on BST64 and a non-ferroelectric oxide such as MgO, $MgTiO_3$, (BST64/$MgTiO_3$ or BST64/MgO) were investigated previously.[7–9] However, most of them were obtained using a conventional solid-state route and interdiffusion evidenced between the two phases led to a decrease of the Curie temperature associated with altered dielectric properties.[10–12] A better control of both losses and interdiffusion was recently achieved with new architectures designed at the nanoscale and synthesized by soft chemistry and solvothermal routes.[13–16] The shaping appears as a critical step in the processing of the final dense composite. Indeed, highly densified ceramics are required for reliable dielectric performances. Thin film composites were recently synthesized.[17–19] In the case of sol–gel structures, a distribution of oriented MgO grains in the BST64 matrix was obtained after film annealing instead of multilayered structure, without any mention of the transition temperature. In polycrystalline films, the crystallinity, defects, and microstructure are hard to control and generate inferior dielectric properties compared with bulk ceramic composites. Thus, ceramic technology currently appears as the method of choice to develop highly reliable materials and by far is largely used for many targeted applications.

To get efficient ferroelectric composites, we propose to improve both architecture and densification. Our strategy consists in (i) limiting the interdiffusion, i.e. reducing the ferroelectric/dielectric interfaces using a multilayer design, and (ii) using spark plasma sintering (SPS) to reach highly densified ceramics while preserving the sandwich architecture. SPS is a very promising tool for nanoceramics sintering and for improving composite materials shaping,[20–23] laminated-based ceramics were indeed recently obtained with no significant diffusion between the different components.[23]

II. Experimental Procedure

(1) Materials and Sintering Process

BST64 nanoparticles of mean diameter close to 50 nm were purchased from Pi-Kem (Tilley, U.K.). MgO (97%) was supplied by Merck (Darmstadt, Germany).

All samples were sintered using a Dr Sinter 2080 SPS apparatus (SPS Syntex Inc., Tokyo, Japan). Precursor's powders (without any sintering aids) were loaded onto an 8-mm inner diameter cylindrical die. The pulse sequence was 12-2 (pulses–dead time or zero current). The temperature was automatically raised to 600°C over a period of 3 min, and from this point it was monitored and regulated by an optical pyrometer focused on a small hole located at the surface of the die. A heating rate of 100°C/min was used to reach the final temperature of 1200°C. Uniaxial pressure of 50 MPa was applied immediately before and until completion of the temperature step at 1200°C. In these conditions, during the sintering cycle, the current passing through the die and the voltage reached maximum values of applied 380 A and 4.4 V, respectively.

(2) Characterization

The microstructure, morphology, and chemical (energy dispersive analysis [EDS]) analyses of the sintered compacts were performed on the sandwiches fracture surface using a scanning electron microscope (JSM 6360A, JEOL, Tokyo, Japan).

Dielectric measurements were performed on discs using a Wayne Kerr component analyzer 6425 (Chichester, U.K.), temperature range 200–500 K, frequency range 100 Hz–100 kHz. The real part of the permittivity derived from the capacitance

Y. Krasik—contributing editor

[†] Author to whom correspondence should be addressed. e-mail: elissald@icmcb-bordeaux.cnrs.fr

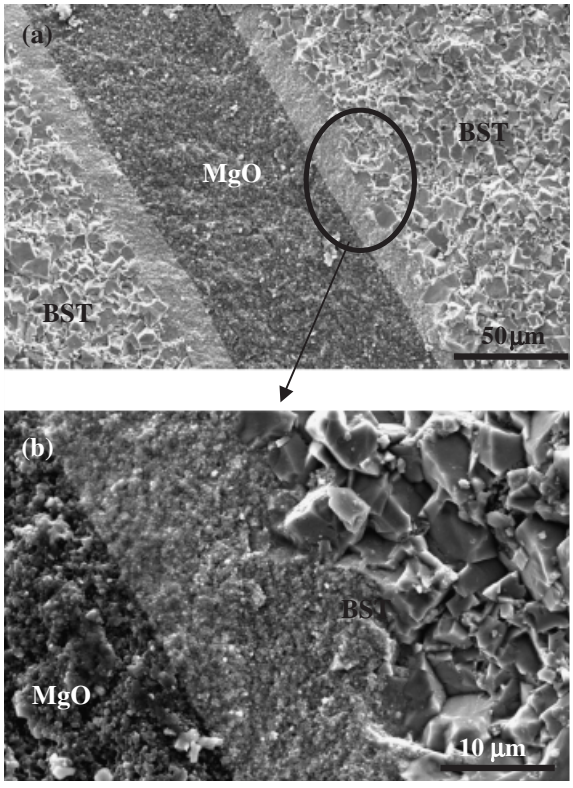

Fig. 1. (a) Scanning electron microscope micrograph of the fracture surface of sandwiched BST64/MgO/BST64 ceramic sintered by spark plasma sintering. (b) Zoom of the BST64/MgO interface showing an intermediate crossover region.

and dielectric losses tan δ (tan $\delta = \varepsilon''_r/\varepsilon'_r$) were directly measured.

III. Results and Discussion

We focused on composites made of BST64 combined with the non-ferroelectric MgO with for main objectives (i) to significantly lower dielectric losses thanks to MgO dielectric performances and (ii) to keep the Curie temperature of the composite close to room temperature while avoiding the interdiffusion of the two phases. Sandwiched BST64/MgO/BST64 multi-layers were prepared by alternatively depositing layers of controlled thickness of ferroelectric and non-ferroelectric oxides (see Section II). A minimum amount of MgO was incorporated in order not to dramatically decrease the dielectric constant of the whole composite. The non-ferroelectric layer plays here the role of barrier to loss. The sintering temperature of BST64 is usually close to 1350°C while densification of MgO requires higher thermal treatment, around 1600°C.[24] Despite different sintering behaviors, dense multilayer ceramic was obtained by SPS (relative density close to 97%). In the SPS process, the combination of high pressure, pulsed electrical current, and plasma generation leads to efficient heat transfer.[25–28] The heating source is not external as the electric current applied passes through the conductive pressurized die containing the powder. Consequently very high heating rates were reached. SPS consolidation leads then to enhanced sintering kinetics and temperature and duration treatment can be significantly reduced compared with conventional sintering. Thus, the interdiffusion of cations from the different layers is limited, allowing the preservation of clean interfaces. The composite was then sintered 3 min at 1200°C with a heating rate of 100°C/mn and applied pressure of 50 MPa. SEM micrograph of the fracture of the sample evidenced

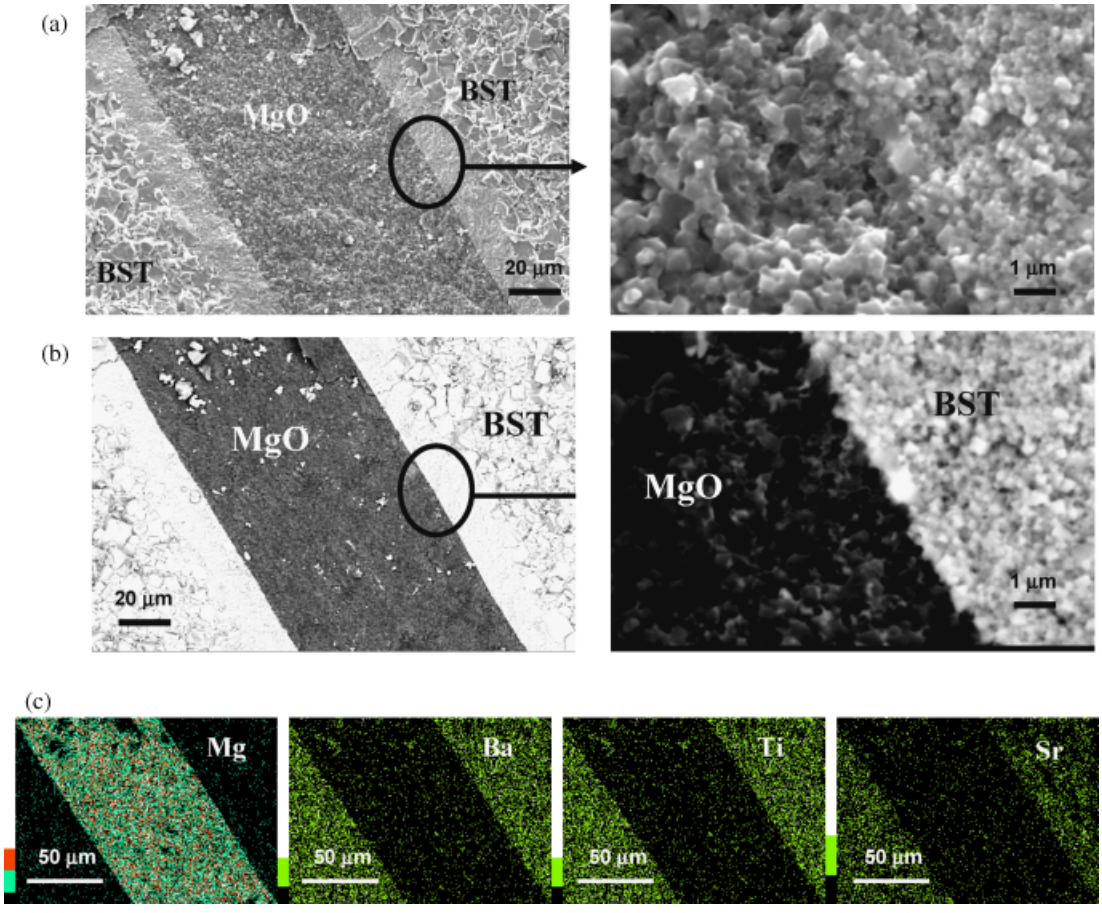

Fig. 2. Scanning electron microscope micrographs (a) and corresponding chemical contrast images (b) of the sandwich and the crossover region which appeared at the BST64/MgO interface. Mapping of the different ionic species confirmed the sharpness of the BST64/MgO interface (c).

particularly sharp and well-defined interfaces between the two components (Fig. 1).

Noteworthy, an intermediate zone appeared in BST64/MgO interface vicinity (Fig. 2(a)). EDS analysis and chemical contrast revealed this crossover region to be made of BST64 (Figs. 2(b) and (c)). A significant difference in microstructure was observed between this intermediate BST64 zone composed of sub-micrometer grains and the remaining micrometric BST64. A fine grain BST64 stripe—about 15 μm thick—was indeed observed on each side of MgO (Fig. 2(a)).

Neither cracks nor increased porosity were observed at the interface reflecting the quality of the as-obtained composites and the absence of strain within the material. However the differences in both cell parameter and thermal dilatation coefficient between BST64 (3.965 Å; 10.5×10^{-6} °C^{-1}) and MgO (4.211 Å, 13.8×10^{-6} °C^{-1}) should lead to tensile and compressive strains, respectively. The crossover region probably plays a key role in relaxing the strains, partly by microstructure adjustment. No similar behaviors were found in the literature in the case of SPS sintering. The pressure contribution was investigated for a better understanding of the intermediate phase formation. When applying the pressure at 600°C instead of 1200°C, the crossover section disappeared with, as a result, a delamination of the composite. Dielectric characterizations of BST64/MgO/BST64 ceramics were performed as a function of temperature and at various frequencies (Fig 3). For comparison, BST64 sintered in the exact same conditions as the sandwich and a BST64 slide cut directly from the composite were dielectrically characterized.

The unmodified Curie temperature provided with a conclusive proof of the absence of interdiffusion. The permittivity anomaly is more diffused; values are lower in the composite but the maximum dielectric temperature is as expected, close to 295 K, which corresponds to that of BST64. At room temperature, the dielectric constant of the multilayer ceramic reached

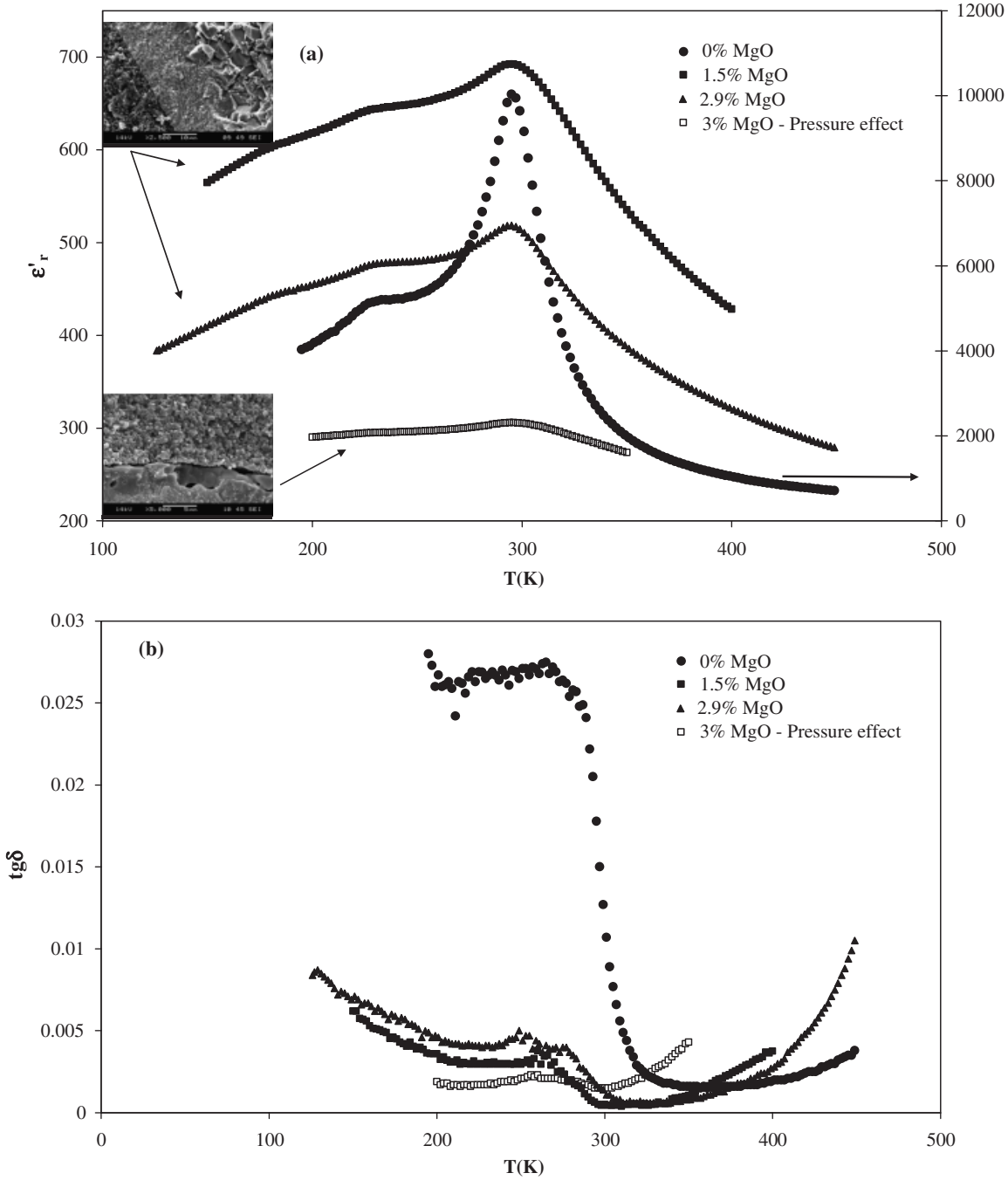

Fig. 3. Dielectric permittivity (a) and losses (b) of spark plasma sintering sintered BST64/MgO/BST64 stack as a function of the thickness ratio MgO/BST64. For sake of comparison, the dielectric permittivity of BST64 alone is also plotted (a, right scale). All data were obtained at 10 kHz.

600 and the thermal sensitivity was significantly reduced compared with that of BST64. Such values strongly depend on the thickness of the non-ferroelectric phase and can be tuned by changing the volume fractions of the two phases. The composite stack effective permittivity of about 500 can be computed with $\varepsilon_{BST} = 8000$, $\varepsilon_{MgO} = 10$ and a thickness ratio of 98/2 between BST64 and MgO. As expected, a decrease of permittivity was observed when increasing the MgO content (Fig. 3). Note that without sharp interfaces between the two phases, the series model used for this permittivity estimate would be meaningless. Changing the pressure parameter in the sintering cycle led to a degradation of both microstructure and dielectric performances (delamination of the sandwich structure, significant decrease of the permittivity). The incorporation of MgO strongly improved the performance of the material in terms of dielectric losses, as the losses in the multilayer capacitor had significantly decreased and lie well below 1% in the whole temperature range.

IV. Conclusion

Highly densified BST64/MgO/BST64 multilayer ceramic was obtained via SPS, which allowed high densification at relatively low temperature and short treatment times compared with conventional sintering. Hence, suppression of interdiffusion between the ferroelectric and the non-ferroelectric phases was possible. As expected, the composite exhibited dielectric losses well below 1% while keeping the Curie temperature of the ferroelectric part unchanged. Both the lower temperature coefficient and the low losses of the stack are key improvements which should be considered for further applications. Such increased performances could be reached thanks to the SPS sintering process.

References

[1]N. Setter and R. Waser, "Electroceramic Materials," *Acta Mater.*, **48**, 151–78 (2000).

[2]Y. Yuan, S. Zhang, and W. You, "Preparation of $BaTiO_3$-Based X7R Ceramics With High Dielectric Constant by Nanometer Oxides Doping Donor," *Mater. Lett.*, **58**, 1959–63 (2004).

[3]G. H. Hertling, "Ferroelectric Ceramics: History and Technology," *J. Am. Ceram. Soc.*, **82** [4] 797–818 (1999).

[4]L. C. Sengupta, E. Ngo, S. Stowell, and M. E. O'Day, "Novel Ceramic Ferroelectric Composite Materials—BSTO–MgO Based Compounds U.S. Patent., 5427988, 1995.

[5]L. C. Sengupta and S. Sengupta, "Breakthrough Advances in Low Loss, Tunable Dielectric Materials," *Mater. Res. Innov.*, **2**, 278–82 (1999).

[6]E. Ngo, P. C. Joshi, M. W. Cole, and C. W. Hubbard, "Electrophoretic Deposition of Pure and MgO Modified $Ba_{0.6}Sr_{0.4}TiO_3$ Thick Films for Tunable Microwave Devices," *Appl. Phys. Lett.*, **79** [2] 248–50 (2001).

[7]E. F. Alberta, A. S. Bhalla, L. Pardo, and R. Jimenez, "Novel BST: $MgTiO_3$ Composites for Frequency Agile Applications," *Ferroelectrics*, **268**, 169–74 (2002).

[8]L. C. Sengupta, "Ceramic Ferroelectric Composite Material BSTO–Magnesium Based Compound U.S. Patent 5635434, 1997.

[9]L. C. Sengupta, S. Sengupta, and E. Ngo, "Multilayered Conformal Coating of Tunable, Low Electronic Loss Ceramic Composites and Method of Production U.S. Patent 6 358 386 (2002).

[10]S. Nenez, A. Morell, M. Paté, M. Maglione, J. C. Niepce, and J. P. Ganne, "Dielectric Properties of Barium Strontium Titanate/Non Ferroelectric Oxide Ceramic Composites," *Key Eng. Mater.*, **206–213**, 1513–8 (2002).

[11]W. Chang and L. Sengupta, "MgO-Mixed $Ba_{0.6}Sr_{0.4}TiO_3$ Ceramics and Thin Films for Tunable Microwave Applications," *J.Appl.Phys.*, **92** [7] 3941–6 (2002).

[12]T. Nagai, K. Iijima, H. J. Hwang, M. Sando, T. Sekino, and K. Niihara, "Effect of MgO Doping on the Phase Transformations of $BaTiO_3$," *J. Am. Ceram. Soc.*, **83**, 107–12 (2000).

[13]V. Hornebecq, C. Huber, M. Maglione, M. Antionetti, and C. Elissalde, "Dielectric Properties of Pure $(BaSr)TiO_3$ and Composites with Different Grain Size: From Nanometer to Micrometer," *Adv. Funct. Mater.*, **14** [9] 899–904 (2004).

[14]S. Mornet, C. Elissalde, V. Hornebecq, O. Bidault, E. Duguet, A. Brisson, and M. Maglione, "Controlled Growth of Silica Shell on $Ba_{0.6}Sr_{0.4}TiO_3$ Nanoparticles Used as Precursors of Ferroelectric Composites," *Chem. Mater.*, **17**, 4530–6 (2005).

[15]C. Aymonier, C. Elissalde, H. Reveron, F. Weill, M. Maglione, and F. Cansell, "Supercritical Fluid Technology of Nanoparticles Coating for New Ceramic Materials," *J. Nanosci. Nanotechnol.*, **5** [6] 980–3 (2005).

[16]H. Y. Tian, J. Q. Qi, Y. Wang, J. Wang, H. L. W. Chan, and C. L. Choy, "Core–Shell Structure of Nanoscaled $Ba_{0.5}Sr_{0.5}TiO_3$ Self-Wrapped by MgO Derived from a Direct Solution Synthesis at Room Temperature," *Nanotechnology*, **16**, 47–52 (2005).

[17]M. Jain, S. B. Majumder, R. S. Katiyar, and D. C. Agrawald, "Dielectric Properties of Sol–Gel–Derived MgO: $Ba_{0.5}Sr_{0.5}TiO_3$ Thin-Film Composites," *Appl. Phys. Lett.*, **81** [7] 3212–4 (2002).

[18]M. Jain, S. B. Majumder, R. S. Katiyar, and A. S. Bhalla, "Novel Barium Strontium Titanate $Ba_{0.5}Sr_{0.5}TiO_3$/MgO Thin Film Composites for Tunable Microwave Devices," *Mater. Lett.*, **57**, 4232–6 (2003).

[19]V. Reymond, D. Michau, S. Payan, and M. Maglione, "Strong Improvement of the Dielectric Losses of $Ba_{0.6}Sr_{0.4}TiO_3$ Thin Films Using a SiO_2 Barrier Layer," *J.Phys.: Conden. Matter*, **16**, 9155–62 (2004).

[20]Z. Zhao, V. Buscaglia, M. Viviani, M. T. Buscaglia, L. Mitoseriu, A. Testino, M. Nygren, M. Johnsson, and P. Nanni, "Grain-Size Effects on the Ferroelectric Behaviour of Dense Nanocrystalline $BaTiO_3$," *Phys. Rev. B*, **70**, 024107–1 (2004).

[21]A. Peigney, "Tougher Ceramics with Nanotubes," *Nat. Mater.*, **2** [1] 15–6 (2003).

[22]G.-D. Zhan, J. Kuntz, J. Wan, and A. K. Mukherjee, "Single-Wall Carbon Nanotubes as Attractive Toughening Agents in Alumina-Based Nanocomposites," *Nat. Mater.*, **2**, 38–42 (2003).

[23]Y. J. Wu, N. Uekawa, and K. Kakegawa, "Sandwiched $BaNd_2Ti_4O_{12}$/$Bi_4Ti_3O_{12}$/$BaNd_2Ti_4O_{12}$ Ceramics Prepared by Spark Plasma Sintering," *Mater. Lett.*, **57**, 4088–92 (2003).

[24]G. S. Upaddhyaya, *Sintered Metallic and Ceramic Materials*. J. Wiley and Sons, New York, 2000.

[25]W. Chen, U. Anselmi-Tamburini, J. E. Garay, J. R. Groza, and Z. A. Munir, "Fundamental Investigations on the Spark Plasma Sintering/Synthesis Process: I. Effect of DC Pulsing on Reactivity," *Mater. Sci. Eng. A*, **394** [1–2] 132–8 (2005).

[26]U. Anselmi-Tamburini, S. Gennari, J. E. Garay, and Z. A. Munir, "Fundamental Investigations on the Spark Plasma Sintering/Synthesis Process: II. Modeling of Current and Temperature Distributions," *Mater. Sci. Eng. A*, **394** [1–2] 139–48 (2005).

[27]U. Anselmi-Tamburini, J. E. Garay, and Z. A. Munir, "Fundamental Investigations on the Spark Plasma Sintering/Synthesis Process: III. Current Effect on Reactivity," *Mater. Sci. Eng. A*, **407** [1–2] 24–30 (2005).

[28]M. Nygren and S. Zhen, "On the Preparation of Bio-, Nano- and Structural Ceramics and Composites by Spark Plasma Sintering," *Solid State Sci.*, **5**, 125–31 (2003). □